NASA Technical Memorandum 4408

Target Fragmentation in Radiobiology

John W. Wilson, Francis A. Cucinotta,
Judy L. Shinn, and Lawrence W. Townsend

FEBRUARY 1993

NASA Technical Memorandum 4408

Target Fragmentation in Radiobiology

John W. Wilson, Francis A. Cucinotta,
Judy L. Shinn, and Lawrence W. Townsend
Langley Research Center
Hampton, Virginia

Abstract

Nuclear reactions in biological systems produce low-energy fragments of the target nuclei seen as local events of high linear energy transfer (LET). A nuclear-reaction formalism is used to evaluate the nuclear-induced fields within biosystems and their effects within several biological models. On the basis of direct ionization interaction, one anticipates high-energy protons to have a quality factor and relative biological effectiveness (RBE) of unity. Target fragmentation contributions raise the effective quality factor of 10 GeV protons to 3.3 in reasonable agreement with RBE values for induced micronuclei in bean sprouts. Application of the Katz model indicates that the relative increase in RBE with decreasing exposure observed in cell survival experiments with 160 MeV protons is related solely to target fragmentation events. Target fragment contributions to lens opacity give an RBE of 1.4 for 2 GeV protons in agreement with the work of Lett and Cox. Predictions are made for the effective RBE for Harderian gland tumors induced by high-energy protons. An exposure model for lifetime cancer risk is derived from NCRP 98 risk tables, and protraction effects are examined for proton and helium ion exposures. The implications of dose rate enhancement effects on space radiation protection are considered.

Introduction

As an energetic-charged particle passes through a region of material, it will suffer many atomic/molecular interactions to which only small amounts of energy are given to ionization/excitation at each interaction site. Secondary electrons and photons propagate the energy from the initial loss site causing a broadening of the particle track (Katz et al. 1971; Chatterjee, Maccabee, and Tobias 1973; Kellerer and Chmelevsky 1975; Paretzke 1988). In this way, the passing particle can affect a localized volume, even though the path is remote to the localized volume itself. Occasionally, the passing energetic particle undergoes a nuclear reaction in which a large amount of its kinetic energy is given to the nucleus of the struck atom. Often, several nuclear disintegration fragments (nuclear stars) are produced of sufficient energy to form well-defined tracks emanating from the interaction site. These fragments may also affect localized volumes remote to the initial particle trajectory.

In the present work, we endeavor to evaluate the field quantities for the nuclear disintegration products formed in nuclear reactions in tissue. We consider explicitly the localized energy deposit associated with the fragments and their resulting impact on biological response in the context of several dose response models. The effect of secondary electrons is studied through the Katz track structure model. All other models used depend only on the density of ionization along the track length. Several biological end points are considered including cell survival, cell transformation, cataract formation, Harderian gland tumors, and cancer risk. Future work will be oriented toward track structure models.

Target Fragment Transport

An expression for ion fluence in a region bounded by a surface $\mathbf{\Gamma}$ (Wilson 1977) is given as

$$\phi_j(\mathbf{x},\mathbf{\Omega},E) = \frac{S_j(E_\gamma)\ P_j(E_\gamma)}{S_j(E)\ P_j(E)}\,\phi_j(\mathbf{\Gamma}_{\Omega,x},\mathbf{\Omega},E_\gamma) + \sum_k \int_E^{E\gamma} dE' \frac{A_j\ P_j(E')}{S_j(E)\ P_j(E)} \int_{E'}^{\infty} dE'' \int d\mathbf{\Omega}'\, r_{jk}(E',E'',\mathbf{\Omega},\mathbf{\Omega}') \times \phi_k\left\{\mathbf{x} + \left[R_j(E) - R_j(E')\right]\mathbf{\Omega},\mathbf{\Omega}',E''\right\} \quad (1)$$

where $E_\gamma = R_j^{-1}[\rho - d + R_j(E)]$, $\rho = \mathbf{\Omega}\cdot\mathbf{x}$, $d = \mathbf{\Omega}\cdot\mathbf{\Gamma}_{\Omega,x}$, and $P_j(E)$ is the total nuclear survival probability. In equation (1), $S(E)$ denotes the stopping power, E denotes the energy, $\mathbf{\Omega}$ denotes the direction of motion, $R_j(E)$ denotes the range, and A_j denotes the atomic mass number of ions of type j. The integral over E' is a summation over the collisional source distribution from the boundary ($E' = E_\gamma$) to the point $\mathbf{x}(E' = E)$. We approximate equation (1) in a perturbation series by taking

$$\phi_k(\mathbf{x}',\mathbf{\Omega}',E'') \approx \frac{S_k(E''_\gamma)\ P_k(E''_\gamma)}{S_k(E'')\ P_k(E'')}\,\phi_k\left(\mathbf{\Gamma}_{\Omega',x'},\mathbf{\Omega}',E''_\gamma\right) \quad (2)$$

where

$$\mathbf{x}' = \mathbf{x} + \left[R_j(E) - R_j(E')\right]\mathbf{\Omega},\ \rho' = \mathbf{\Omega}'\cdot\mathbf{x}',\ d' = \mathbf{\Omega}'\cdot\mathbf{\Gamma}_{\Omega'x'},\ \text{and}\ E''_\gamma = R_k^{-1}\left[\rho' - d' + R_k(E'')\right]$$

We specialize to a unidirectional monoenergetic beam of type M particles at the boundary as

$$\phi_k(\mathbf{\Gamma},\mathbf{\Omega},E) = \delta_{kM}\ \delta(E - E_o)\ \delta(\mathbf{\Omega} - \mathbf{\Omega}_o) \quad (3)$$

for which equation (1) may be simplified to

$$\phi_j(\mathbf{x},\mathbf{\Omega},E) = e^{-\sigma_j(\rho-d)}\frac{Sj(E\gamma)}{S_j(E)}\delta_{jM}\ \delta(E_\gamma - E_o)\ \delta(\mathbf{\Omega} - \mathbf{\Omega}_o) + \int_E^{E_\gamma} dE' \frac{A_j}{S_j(E)} \exp\left\{-\sigma_j\left[R_j(E') - R_j(E)\right]\left[-\sigma_m(\rho' - d')\, r_{jM}(E',E''_o,\mathbf{\Omega},\mathbf{\Omega}_o)\right]\right\} \quad (4)$$

where $E''_o = R_k^{-1}[R_k(E_o) - \rho' + d']\sigma_j$ is the nuclear macroscopic cross section and r_{jM} is the corresponding fragmentation cross section. If we restrict ourselves to a small volume of material ($\sigma_j(\rho - d) < 0.01$ corresponding to a few to several millimeters), then

$$\phi_j(\mathbf{x},\mathbf{\Omega},E) = \frac{S_j(E_\gamma)}{S_j(E)}\delta_{jM}\ \delta(E_\gamma - E_o)\ \delta(\mathbf{\Omega} - \mathbf{\Omega}_o) + \int_E^{E_\gamma} dE' \frac{A_j}{S_j(E)}\left[r^P_{jM}(E',E''_o,\mathbf{\Omega},\mathbf{\Omega}_o) + r^T_{jM}(E',E''_o,\mathbf{\Omega},\mathbf{\Omega}_o)\right] \quad (5)$$

where the projectile and target fragment terms are shown separately. The projectile term has a contribution only at energies near E_o, whereas the target term has a contribution only for $E \ll E_o$. At high energy we have

$$E_\gamma \approx E + \frac{1}{A_j}S_j(E)\ (\rho - d) \quad (6)$$

in which case

$$\phi_j(\mathbf{x},\mathbf{\Omega},E) \approx \delta_{jM}\ \delta(E-E_o)\ \delta(\mathbf{\Omega}-\mathbf{\Omega}_o) + r^P_{jM}(E,E_o,\mathbf{\Omega},\mathbf{\Omega}_o)\ (\rho-d) + \int_E^{E_\gamma} dE' \frac{A_j}{S_j(E)} r^T_{jM}(E',E_o,\mathbf{\Omega},\mathbf{\Omega}_o) \tag{7}$$

The absorbed energy density is then

$$D(\mathbf{x}) = \sum_j \int_0^\infty dE \int d\mathbf{\Omega}\ S_j(E)\ \phi_j(\mathbf{x},\mathbf{\Omega},E)$$

$$= S_M(E_o) + \sum_j S_j(E_o)\ m^P_{jM}\ \sigma_M(\rho-d)$$

$$+ \sum_j \int_0^\infty A_j\ dE \int_E^{E_\gamma} dE'\ r^T_{jM}(E',E_o,\mathbf{\Omega},\mathbf{\Omega}_o) \tag{8}$$

The first term clearly dominates the second (that is, $[\sigma_M(\rho-d) < 0.01$ and $S_M(E_o) \gg \sum_j S_j(E_o)\ m^P_{jM}]$). The fact that the third term is nonnegligible results from the large stopping power of the low-energy fragments represented by the third term compared with $S_M(E_o)$, which also results in all their energy being deposited locally (Wilson 1977). On this basis, equation (7) may be reduced to

$$\phi_j(\mathbf{x},\mathbf{\Omega},E) \approx \delta_{jM}\ \delta(E-E_o)\ \delta(\mathbf{\Omega}-\mathbf{\Omega}_o) + \int_E^{E_\gamma} dE' \frac{A_j}{S_j(E)}\ r^T_{jM}(E',E_o,\mathbf{\Omega},\mathbf{\Omega}_o) \tag{9}$$

Accordingly, the high-energy beam exposure of a small object can be treated by evaluating the direct ionization of the primary particles and the transport of low-energy fragments produced uniformly throughout the volume. This treatment is represented in equation (9). We now consider some applications of target fragment transport.

Effects in Conventional Risk Assessment

Biological risks are related to the local energy deposited by the passage of energetic ions. The ionization energy loss, the ($S_M(E_o)$ term of eq. (8)), is on the order of $0.2Z^2$ keV/μm for a passing relativistic ion of charge Z. Some ions produce nuclear reactions in which 10 to 100 MeV (per event) are released (Wilson, Stith, and Stock 1983) locally as secondary nuclear fragments (the third term of eq. (8)). The average energy transfer rate is approximately $0.05A^{2/3}$ keV/μm, where A is the ion atomic weight. Because the quality factor of the fragments is usually taken as 20, the risk associated with direct atomic ionization is on the order of the risk associated with the nuclear events for incident low-charge ions ($Z < 5$), whereas the risk is dominated by the direct ionization for high charge ($Z \gg 5$). At a sufficiently low energy, the direct ionization always dominates the biological risk independent of the ion charge and mass. In the present section, we quantify these various contributions to biological risk using quality factors presently in force (ICRP 26 in Anon. 1987) and evaluate the effects of newly proposed quality factors (ICRU 40 in Anon. 1986; ICRP 60 in Anon. 1991).

We consider a volume of tissue through which a monoenergetic ion fluence $\phi_z(E_p)$ of energy E_p has passed and evaluate the energy absorbed by the media in the passage. Several processes exist by which the ion gives up energy to the media: electronic excitation/ionization, nuclear coulomb scattering, nuclear elastic scattering, and nuclear reaction. The electronic excitation/ionization is contained in the stopping power that is evaluated by methods discussed in relation to equation (8) (Wilson et al. 1984). The nuclear coulomb elastic scattering is highly peaked at low-momentum transfer, and the energy transfers per event of a few hundred eV or less are typical (Wilson et al. 1983). The nuclear elastic scattering energy transfer is on the order of 1 MeV or less and can be neglected in comparison with reactive processes. A model for proton-induced reactions in tissue constituents has been given elsewhere (Wilson et al. 1988, 1989) and will provide the basis for the present evaluation.

The secondary-particle radiation fields $\phi_j(E)$ are given as

$$\phi_j(E) = \frac{1}{S_j(E)} \int_E^\infty \zeta_j(E')\, dE' \tag{10}$$

where $S_j(E)$ is the stopping power and $\zeta_j(E)$ is the particle source energy distribution, which is given as

$$\zeta_j(E) = \rho\ \sigma_j(E_p)\ \ f_j(E)\ \ \phi_Z(E_p) \tag{11}$$

where ρ is the nuclear density, $\sigma_j(E_p)$ is the fragmentation cross section, and $f_j(E)$ is the fragment spectrum as discussed elsewhere (Wilson, Townsend, and Khan 1989). The total absorbed energy is approximately

$$D_Z(E_p) = S_Z(E_p)\ \ \phi_Z(E_p) + \sum_j \int_0^\infty S_j(E)\ \ \phi_j(E)\ \ dE \tag{12}$$

Equation (12) may be written as

$$D_Z(E_p) = S_Z(E_p)\ \ \phi_Z(E_p) + E_j\ \sigma_j(E_p)\ \ \rho\ \phi_Z(E_Z) \tag{13}$$

where E_j is the average energy associated with each spectral distribution $f_j(E)$. Similarly, the dose equivalent is

$$\begin{aligned} H_Z(E_p) = {} & Q_Z(E_p)\ \ S_Z(E_p)\ \ \phi_Z(E_p) \\ & + \sum_j \overline{Q}_{F_j} E_j\ \sigma_j(E_p)\ \ \rho\ \phi_Z(E_p) \end{aligned} \tag{14}$$

where $\overline{Q}_{F_j}$ is the spectral-averaged quality factor of the jth secondary particle (Shinn, Wilson, and Ngo 1990). The sum over j will include the usual "evaporation" products, including the low-energy protons.

Evaluation of Dose Equivalent

We now evaluate equation (14) for the conventional quality factor $Q(L)$ that is dependent on linear energy transfer (LET) (ICRP 26 in Anon. 1987; ICRP 60 in Anon. 1991) and the lineal-energy-dependent quality factor $Q(y)$ that was recently proposed (ICRU 40 in Anon. 1986). To implement $Q(y)$, we used appendix B of ICRU 40 in which the lineal energy distributions are assumed to be linearly dependent on y at a fixed LET. Some problems of this assumption have been discussed by Townsend, Wilson, and Cucinotta (1987), which we circumvent herein by

Table 1. Spectral-Averaged Quality Factor for Individual Isotopes Produced in 1-GeV Proton-Induced Reactions in ^{16}O

Z_j	A_f	E_j, MeV	$\overline{Q}_{F_j}$		
			ICRP 26	ICRU 40	ICRP 60
1	1	8.69	2.73	3.71	2.65
1	2	10.70	4.09	5.87	4.36
1	3	10.40	5.20	7.72	6.07
2	3	11.20	12.38	19.52	17.86
2	4	12.30	13.90	21.88	20.16
3	6	6.85	19.25	23.19	20.03
3	7	6.16	19.50	22.38	19.20
4	9	4.79	19.77	15.14	15.06
4	10	4.11	19.73	14.95	15.01
5	9	4.79	19.81	11.47	13.02
5	10	4.11	19.78	11.54	13.06
5	11	3.71	19.75	11.88	13.26
5	12	2.74	19.70	12.58	13.70
6	11	3.71	19.79	9.96	12.03
6	12	2.74	19.75	10.71	12.48
6	13	2.05	19.68	11.96	13.28
6	14	1.34	19.56	14.11	14.53
6	15	0.69	19.17	18.30	17.06
7	13	2.05	19.74	10.53	12.32
7	14	1.37	19.64	12.61	13.62
7	15	0.69	19.35	16.73	16.14
8	15	0.69	19.45	15.50	15.35

assuming $Q \geq 1$. The spectral-averaged quality factors of the conventional method (ICRP 26 in Anon. 1987; ICRP 60 in Anon. 1991) and proposed method (ICRU 40 in Anon. 1986) are shown in table 1 for the various isotopes produced in ^{16}O reactions. The proposed values are generally greater than the conventional values, except for the heavier fragments where the proposed values are substantially smaller. The conventional average quality factors show, generally, a weak isotope dependence, whereas the proposed average quality factors show a strong isotope dependence with neutron-rich isotopes being the most biologically damaging.

Results and Discussion

The dose equivalent per unit fluence of incident ions of charge Z and energy per nucleon E_p are shown in figures 1 to 3. Figure 1 is based on current quality factors (ICRP 26 in Anon. 1987), figure 2 is based on newly proposed quality factors (ICRU 40 in Anon. 1986), and figure 3 is based on newly recommended values (ICRP 60 in Anon. 1991). The proton-induced fragmentation cross sections are taken from Wilson, Townsend, and Khan (1989). The proton cross sections are velocity-scaled according to the proposed factorization model of Lindstrom et al. (1975) as modified by Silberberg, Tsao, and Shapiro (1976). The limitations of this model, as discussed elsewhere (Wilson et al. 1984), do not concern us here because the ^{16}O and ^{12}C ion beam data were used in the original derivation by Lindstrom et al. (1975), which was retained in subsequent modifications of Silberberg, Tsao, and Shapiro (1976), and adequately represent the ^{16}O and ^{12}C data. The problems with this scaling model arise for nuclear fragmentation predictions far removed from projectile-target combinations used in fitting the model parameters. For example, there are no light-fragment data for iron fragmentation with which to fit the model (Wilson, Townsend, and Badavi 1987), but such experiments are currently in progress. The

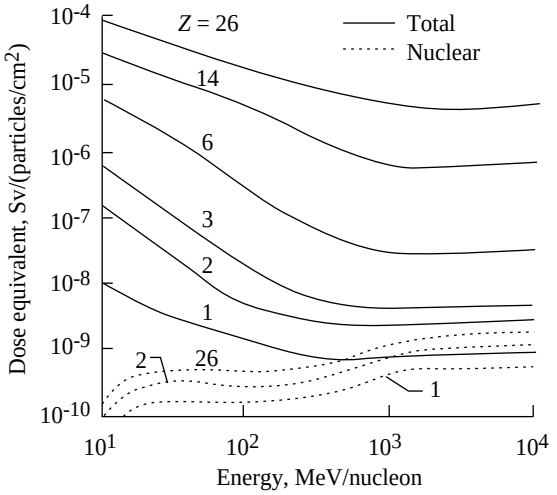

Figure 1. Dose equivalent of various ion types including nuclear reactions for ICRP 26 quality factor (Anon. 1987).

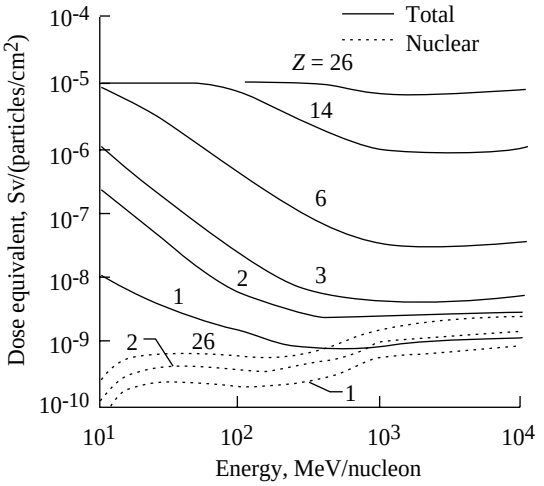

Figure 2. Dose equivalent of various ion types including nuclear reactions for ICRU 40 quality factor (Anon. 1986).

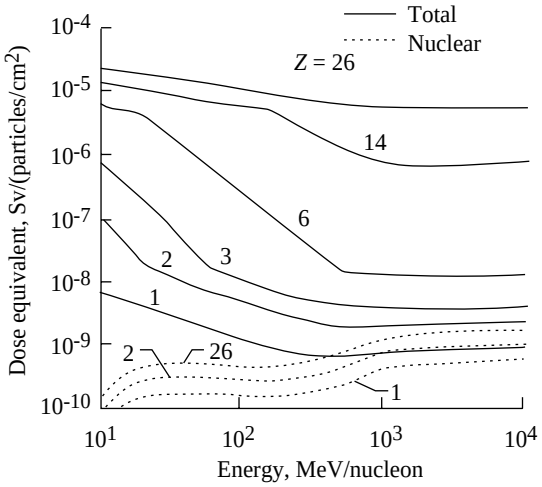

Figure 3. Dose equivalent of various ion types including nuclear reactions for ICRP 60 quality factor (Anon. 1991).

50-percent increase proposed for the ^{20}Ne data is within the uncertainty generally regarded for the Silberberg, Tsao, and Letaw (1983) parameterization. (See also Mathews (1983).)

The nuclear contribution to the dose equivalent increases rapidly at the lowest energies as new channel thresholds are passed with increasing energy opening new reaction mechanisms. Only a small variation is seen between 20 and 300 MeV/nucleon and this is related to nuclear transparency (Townsend, Wilson, and Bidasaria 1982). New inelastic channels open above the pion production threshold and cause a rapid rise in dose equivalent above 300 MeV/nucleon. The fractional contribution of nuclear reaction effects is shown in table 2 for the two quality factors and ion types shown in figures 1 to 3 at 10 GeV/nucleon. The nuclear contribution to dose equivalent for C and heavier ions is less than 5 percent. Nuclear contributions for lighter ions can be substantial and as high as 70 percent.

The average quality factors including nuclear reaction effects are shown in figures 4 to 6. The nuclear effects are clearly seen as the rise in average quality factor at high energies, especially

Table 2. Fractional Contribution of Nuclear Reactions to Total Dose Equivalent at 10 GeV/nucleon for ICRP 26, ICRU 40, and ICRP 60 Quality Factors.

Report	Fractional contribution for projectile—						
	^{1}H	^{4}He	^{3}Li	^{9}Be	^{12}C	^{28}Si	^{56}Fe
ICRP 26	0.59	0.43	0.27	0.17	4.2×10^{-2}	2.5×10^{-3}	3.8×10^{-4}
ICRU 40	.70	.51	.34	.21	4.7	2.1	3.5
ICRP 60	.66	.46	.30	.19	4.6	2.1	3.5

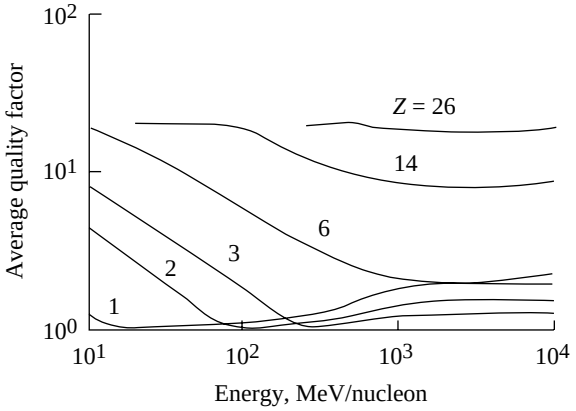

Figure 4. Average quality factor of various ion types including nuclear reactions for ICRP 26 quality factor (Anon. 1977).

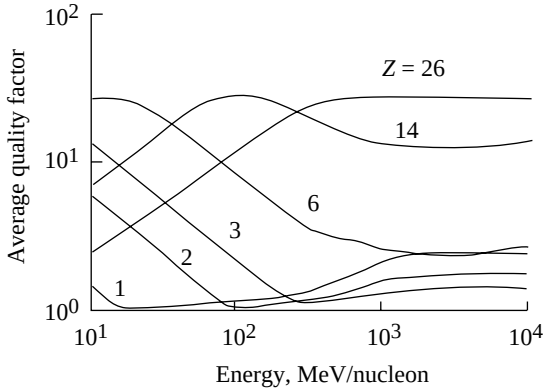

Figure 5. Average quality factor of various ion types including nuclear reactions for ICRU 40 quality factor (Anon. 1986).

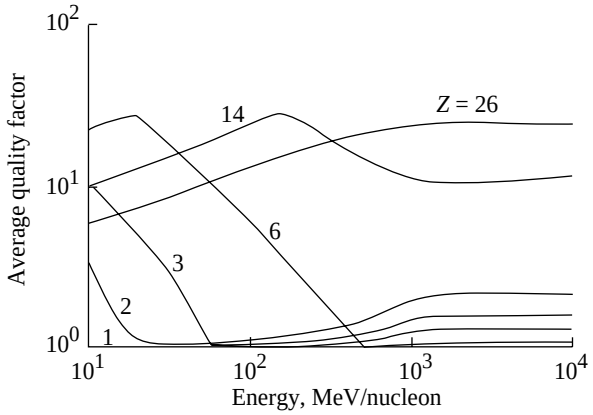

Figure 6. Average quality factor of various ion types including nuclear reactions for ICRP 60 quality factor (Anon. 1991).

for the light ions. The increase in average quality factors for high-energy protons of ICRU 40 (Anon. 1986) compared with the value obtained for ICRP 26 (Anon. 1987) is only 25 percent. Consequently, the earlier estimates of Alsmiller, Armstrong, and Coleman (1970), in which the quality factor of 20 is assumed for all nuclear fragments of mass greater than 1 amu (atomic mass unit), are expected to remain slightly conservative with respect to biological risk, even if the ICRU 40 (Anon. 1986) quality factor is enforced.

We now cite a few experiments that have measured relative biological effectiveness (RBE) for some biological end points. A genetic change in radiation-exposed seeds of maize produces a yellow-green streak in the leaves of the growing plant. The measured RBE for 28 GeV protons yielded an average of 4.4 (Smith 1967). The emergence rate of exposed brine shrimp was studied using 645 MeV and 9.2 GeV protons for which RBE values of 2.3 and 1.5 were reported (Gaubin et al. 1979). A third experiment on micronuclei induction in bean roots by 250 GeV protons found RBE's of 1.8 to 2.1 (Diehl-Marshall and Bianchi 1981). A fourth experiment showed much more dramatic bone marrow depression in primates with 400 MeV protons compared with 32 and 55 MeV protons of energy (Conklin and Hagan 1987). Although evidence exists of RBE being greater than unity because of target fragment effects, cancer induction in humans is not clearly represented by the quality factors presented herein.

Effects on Cellular Track Models

The cellular track model of Katz has been described extensively (Katz et al. 1971, 1972, 1986). Here, we outline its basic concepts and consider the extension to the mixed-radiation field seen in space. The biological damage from passing ions is caused by delta-ray production. Cell damage is separated into a so-called grain-count regime (where damage occurs randomly along the ion path) and a track-width regime (where the damage is said to be distributed like a "hairy rope"). The response of the cells is described by four cellular parameters, two of which (m, the number of targets per cell, and D_o, the characteristic X-ray dose) are extracted from the response of the cellular system to X-ray or γ-ray irradiation. The other two parameters (Σ_o, interpreted as the cross-sectional area of the cell nucleus within which the damage sites are located, and κ, a measure of size of the damage site) are found from survival measurements with track-segment irradiations by energetic-charged particles. The transition from the grain-count regime to the track-width regime takes place at $Z^{*2}/\kappa\beta^2 \approx 4$, where Z^* is the effective charge and β is the velocity. The grain-count regime occurs at lower values of $Z^{*2}/\kappa\beta^2$, and the track-width regime occurs at the higher values.

To accommodate for the capacity of cells to accumulate sublethal damage, two modes of inactivation are identified: ion kill (intratrack) and gamma kill (intertrack). For cells damaged by the passage of a single ion, the ion-kill mode occurs. The fraction of cells damaged in the ion-kill mode is taken as $P = \Sigma/\Sigma_o$, where Σ is the single-particle inactivation cross section and P is the probability of the damage in the ion-kill mode. Cells not damaged in the ion-kill mode can be sublethally damaged by the delta rays from the passing ion and then inactivated in the gamma-kill mode by cumulative addition of sublethal damage caused by delta rays from other passing ions. The surviving fraction of a cellular population N (whose response parameters are m, D_o, Σ_o, and κ) after irradiation by a fluence of particles F (Katz et al. 1971) is written as

$$\frac{N}{N_o} = \pi_i \times \pi_\gamma \tag{15}$$

where the ion-kill survivability is

$$\pi_i = e^{-\Sigma F} \tag{16}$$

and the gamma-kill survivability is

$$\pi_\gamma = 1 - \left(1 - e^{-D_\gamma/D_o}\right)^m \tag{17}$$

The gamma-kill dose is

$$D_\gamma = (1 - P)\, D \tag{18}$$

where D is the absorbed dose. The single-particle inactivation cross section is given by

$$\Sigma = \Sigma_o \left[1 - \exp\left(-Z^{*2}/\kappa\beta^2\right)\right]^m \tag{19}$$

where the effective charge number is

$$Z^* = Z\left[1 - \exp\left(-125\beta/Z^{2/3}\right)\right] \tag{20}$$

In the track-width regime where $P > 0.98$, we take $P = 1$.

For cell transformation, the fraction of transformed cells per surviving cell is

$$T = 1 - \left(N'/N'_o\right) \tag{21}$$

where N'/N'_o is the fraction of nontransformed cells, and a set of cellular response parameters for transformations m', D'_o, Σ'_o, and κ' are used. The RBE at a given survival level is given by

$$\text{RBE} = D_X/D \tag{22}$$

where

$$D_X = -D_o\ \ln\left\{1 - \left[1 - (N/N_o)\right]^{1/m}\right\} \tag{23}$$

is the X-ray dose at which this level is obtained. Equations (15) through (23) represent the cellular track model for monoenergetic particles. Mixed-radiation fields have been considered previously in the Katz model. (See, for example, Katz, Sharma, and Homayoonfar 1972.) Next, we consider placing the model in terms of the particle fields described previously.

Evaluation of the Katz Model

The target fragmentation fields are found in closed form in terms of the collision density (Wilson 1977) because these ions are of relatively low energy. Away from any interfaces, the target fields are in a local equilibrium and may be written as

$$\phi_\alpha\left(x, E_\alpha; E_j\right) = \frac{1}{S_\alpha\left(E_\alpha\right)} \int_{E_\alpha}^{\infty} \frac{d\sigma_{\alpha j}\left(E', E_j\right)}{dE'}\ \phi_j\left(x, E_j\right)\ dE' \tag{24}$$

where the subscript α labels the target fragment type, $S_\alpha(E)$ denotes the stopping power, and E_α and E_j are in units of MeV.

The particle fields of the projectiles and target fragments determine the level and type of radiological damage at the end point of interest. The relationship between the fields and the cellular response is now considered within the Katz cellular track model.

The ion-kill term now contains a projectile term as well as a target fragment term as

$$(\Sigma F) = \Sigma_j\left(E_j\right)\ \phi_j\left(x, E_j\right) + \sum_\alpha \int_0^\infty dE_\alpha\ \phi_\alpha\left(x, E_\alpha; E_j\right)\ \Sigma_\alpha\left(E_\alpha\right) \tag{25}$$

whereas the corresponding gamma-kill dose becomes

$$\begin{aligned} D_\gamma = {} & \left[1 - P_j\left(E_j\right)\right]\ S_j\left(E_j\right)\ \phi_j\left(x, E_j\right) \\ & + \sum_\alpha \int_0^\infty dE_\alpha \left[1 - P_\alpha\left(E_\alpha\right)\right]\ S_\alpha\left(E_\alpha\right)\ \phi_\alpha\left(x, E_\alpha; E_j\right) \end{aligned} \tag{26}$$

Use of equations (24) and (25) allows one to define an effective cross section as

$$\Sigma_j^* (E_j) = \Sigma_j (E_j) + \sum_\alpha \int_0^\infty dE_\alpha \frac{\Sigma_\alpha (E_\alpha)}{S_\alpha (E_\alpha)} \int_{E_\alpha}^\infty dE' \frac{d\sigma_{\alpha j} (E', E_j)}{dE'} \tag{27}$$

The first term of equation (27) is caused by the direct ionization of the media by the passing ion of type j. The second term results from target fragments produced in the media.

Results and Discussion

Katz (Waligórski, Sinclair, and Katz 1987) has obtained cellular parameters for survival and neoplastic transformations of C3H10T1/2 from the experiments of Yang et al. (1985) as given in table 3. We note the large uncertainties in the transformation data of Yang, which should lead to a similar uncertainty in the transformation parameters. Parameter sets were found from data for instantaneous and delayed plating of the cells after the irradiation. Here, only the delayed plating case is considered. General agreement with the measured RBE values (Waligórski, Sinclair, and Katz 1987) was found using these parameter sets.

Table 3. Cellular Response Parameters for C3H10T1/2 Cells

Cell-damage type	Values for response parameters—			
	m	D_o, cGy	Σ_o, cm^2	κ
Killing	3	280	5.0×10^{-7}	750
Transformation	2	26 000	1.15×10^{-10}	750

The single-particle inactivation cross sections neglecting target fragmentation of equation (27) are shown in figures 7 and 8 for cell death and transformation, respectively, as a function of the energy (in MeV/amu) of the passing ion. The target fragmentation contribution (the second term of eq. (27)) for protons has been evaluated as shown in figures 9 and 10. For protons, the effect of the target fragments (dashed line, the second term in eq. (27)) dominates over the proton direct ionization (dotted line) at high energy. For high-LET particles (low energy), the direct ionization dominates and target fragmentation effects become negligible. A simple scaling by $\sqrt{A_j}$ relates the proton target fragment term to ions of mass A_j. The resulting effective action cross sections for cell kill and transformation are plotted in figures 11 and 12, respectively. We note that the low-energy ^{56}Fe component of the GCR spectra extends into the track-width regime where $\Sigma > \Sigma_o$, and it is not represented in the present calculation. The error introduced by the present calculation is small.

The RBE is found in the Katz model through equation (22) and has a functional relationship to dose (Cucinotta et al. 1991a, 1991b; Katz and Cucinotta 1991) given in the low dose limit as

$$\text{RBE} = D_o \left(\frac{\Sigma}{\text{LET}} \right)^{1/m} D\,[(1/m) - 1] \tag{28}$$

The implications of equation (28) on space exposure are discussed elsewhere (Cucinotta et al. 1991a). We might ask if the high-LET components of proton exposure show similar characteristics. The RBE for cell survival of Chinese hamster cells exposed to 160 MeV protons was studied by Hall et al. (1978), and their results (dashed curve) are compared with the present model (solid curve) in figure 13. We note that the RBE, without accounting for target

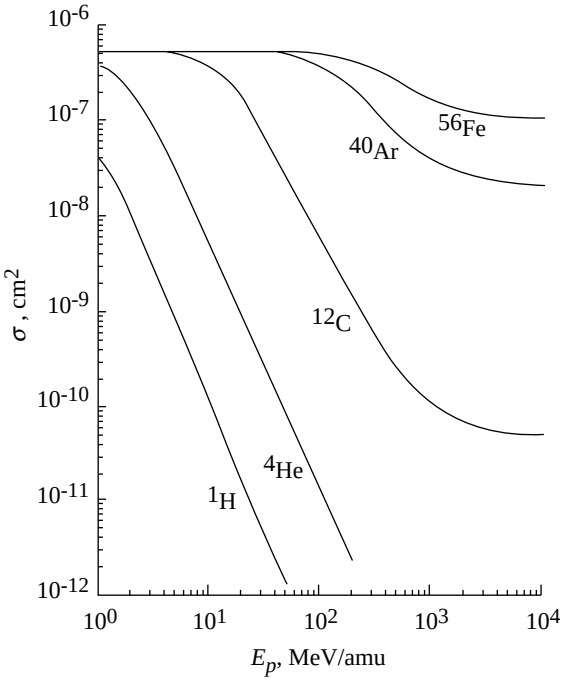

Figure 7. Cell killing cross sections for several ions in C3H10T1/2 cells according to Katz model. Ionization effects only.

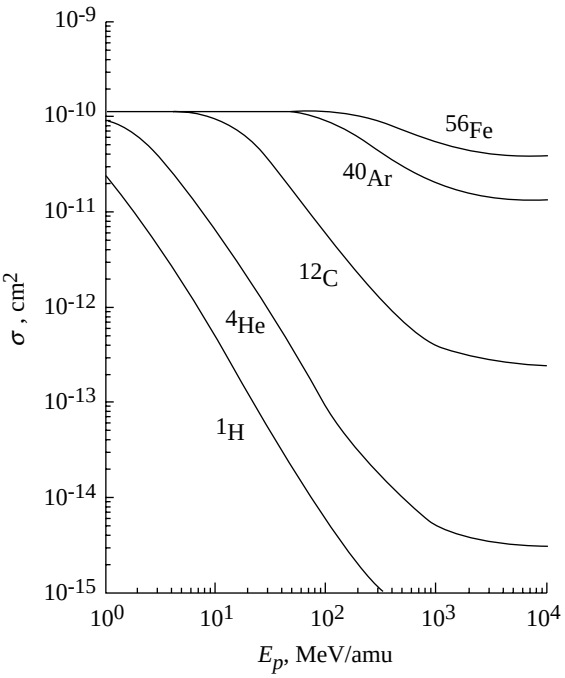

Figure 8. Cell transformation cross sections for several ions in C3H10T1/2 cells according to Katz model. Ionization effects only.

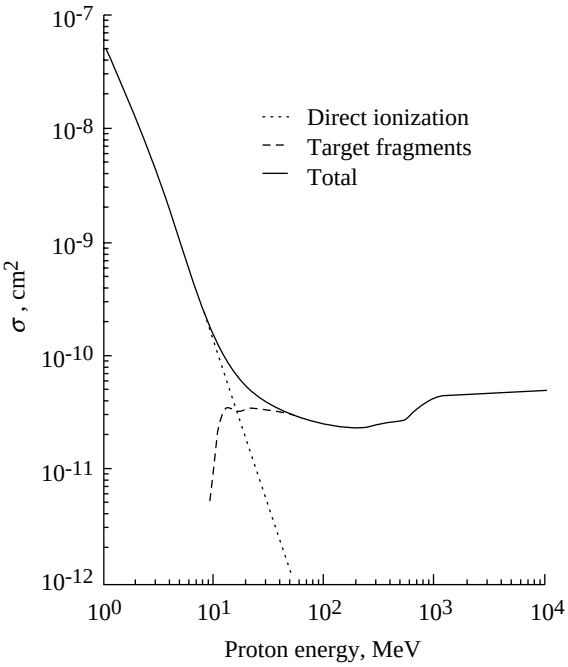

Figure 9. Cell killing cross sections including effects of nuclear reaction effects for protons in C3H10T1/2 cells according to Katz model.

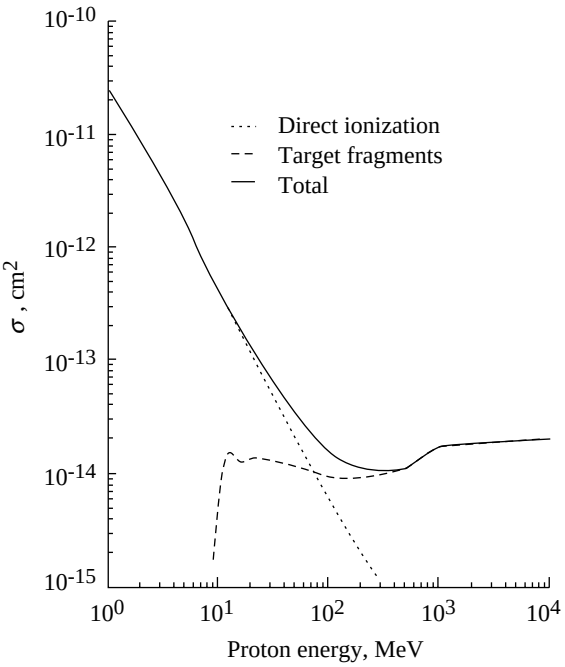

Figure 10. Cell transformation cross sections including nuclear reaction effects for protons in C3H10T1/2 cells according to Katz model.

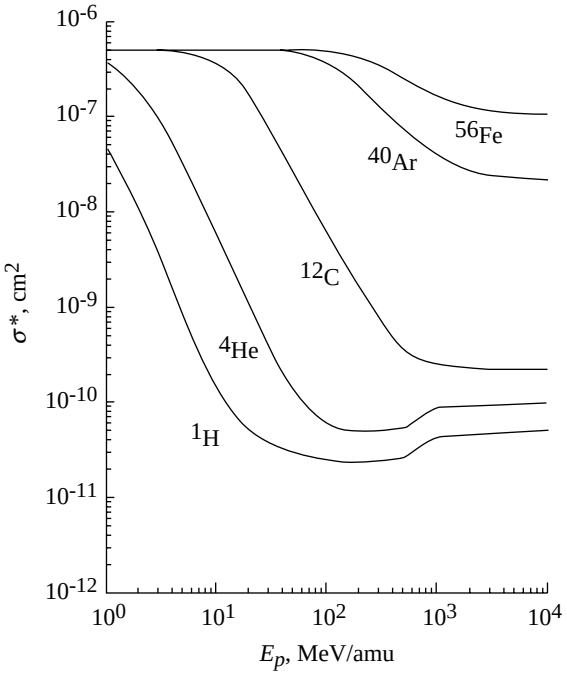

Figure 11. Cell killing cross sections including nuclear reaction effects for various ions in C3H10T1/2 cells.

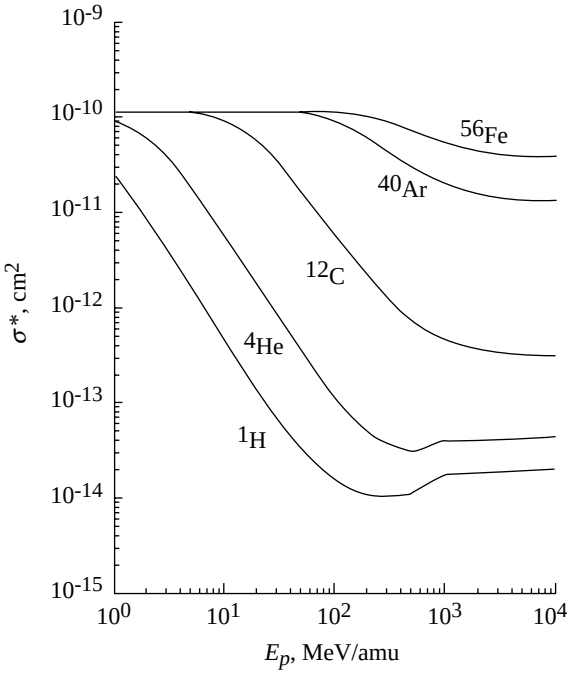

Figure 12. Cell transformation cross sections including nuclear reaction effects for various ions in C3H10T1/2 cells.

fragmentation, remains near unity (dotted curve in fig. 13), and the rise in RBE observed at low doses is solely connected to the target fragments. (Compare with fig. 9.)

Effects on Fluence-Related Risk Coefficients

Harderian Gland Tumors

The idea underlying the concept of risk per unit fluence has been used by researchers for ion exposure (Todd 1964; Curtis, Dye, and Sheldon 1965). The fluence-related risk coefficient F_j is defined as the probability of a given end point of interest (e.g., cancer) per unit fluence of type j particles passing through the organ (Curtis et al. 1992). A first estimate of $F_j(L_j)$ can be found from the RBE values of Fry et al. (1985, 1986) as approximated (Wilson et al. 1991a, 1991b) by

$$\text{RBE} = 0.95 + \frac{a_1}{L}\left(1 + 2e^{-L/14}\right)\left[1 - \exp\left(-a_2 L^2 - a_3 L^3\right)\right] \tag{29}$$

where $a_1 = 18\,720$, $a_2 = 7.43 \times 10^{-6}$, and $a_3 = 1.14 \times 10^{-8}$. (See fig. 14.) Using Curtis et al. (1992) and Wilson et al. (1991a, 1991b), the relation

$$F_j\left(L_j\right) = \frac{\text{RBE}\left(L_j\right)\ L_j}{12.5 D_o} \tag{30}$$

represents the risk coefficient for direct ionization only because RBE was taken as unity for ^{60}Co gamma rays.

In addition to the ionization caused directly by primary and high-energy secondary nuclei from fragmentation of the primary ions, the nuclei constituting biological tissue (i.e., the "target"

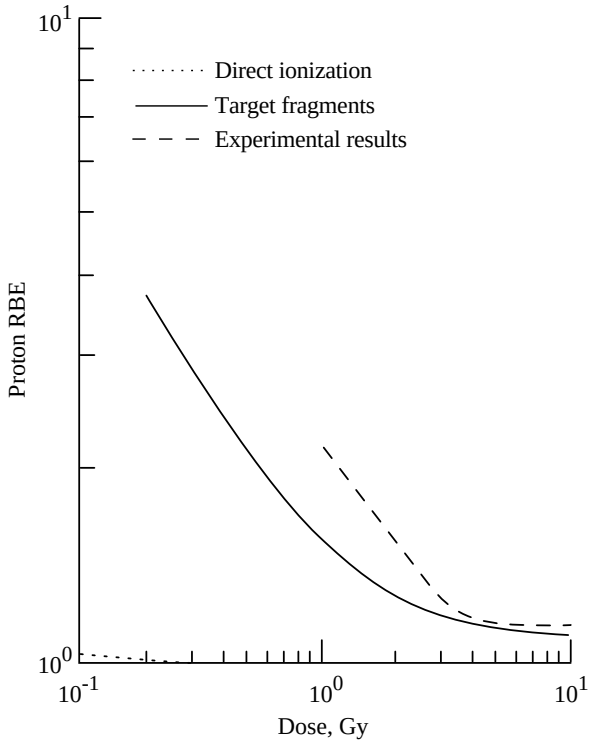

Figure 13. RBE predicted by Katz model for direct ionization and including target fragmentation in comparison with experimental results.

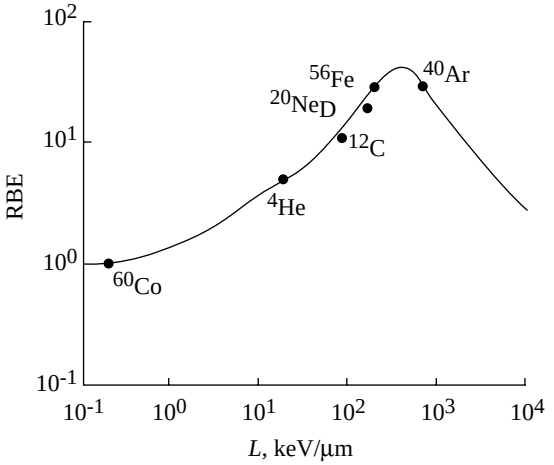

Figure 14. Relative biological effectiveness (RBE) for Harderian gland tumors as function of linear energy transfer.

nuclei) will break up into lower energy and, in some cases, very highly ionizing target fragments. Target fragment fluences $\phi_j(E_j)$, produced by a passing energetic ion of energy E_j, are given by

$$\phi_j\left(E_j\right) = \frac{1}{L_j\left(E_j\right)} \int_{E_j}^{\infty} \sigma_j\left(E_i\right)\ f_j\left(E_j', E_i\right)\ \phi_i\left(E_i\right)\ dE_j' \tag{31}$$

where $\sigma_j(E_i)$ is the macroscopic fragmentation cross section, $f_j(E_j', E_i)$ is the energy distribution of the jth fragment, and $\phi_i(E_i)$ is the fluence of passing ions of energy E_i. The total prevalence at low exposure is given in terms of F_i as

$$P = F_i\left(L_i\right)\ \phi_i\left(E_i\right) + \sum_j \int_0^{\infty} F_j\left[L_j\left(E_j\right)\right]\ \phi_j\left(E_j\right)\ dE_j \tag{32}$$

An effective $F_i^*(L_i)$ using equation (32) is defined as

$$F_i^*\left(L_i\right) = F_i\left(L_i\right) + \sum_j \int_0^{\infty} dE_j \frac{\overline{F}_j\left[\overline{L}_j\left(E_j\right)\right]}{L_j\left(E_j\right)} \int_{E_j}^{\infty} dE_j'\ \sigma_j\left(E_i\right)\ f_j\left(E_j', E_i\right) \tag{33}$$

The effective risk coefficient F_i^* is shown in figure 15 as a function of particle energy for representative charge components with the target fragment contributions shown separately. The nuclear contribution to the effective risk coefficient is reasonably approximated by

$$F_{n_i}^*\left(L_i\right) = A^{0.4}\left\{\frac{2.0 \times 10^{-3}}{1 + \exp\left[-\left(E - 12\right)/4.5\right]} + \frac{1.1 \times 10^{-3}}{1 + \exp\left[-\left(E - 700\right)/363\right]}\right\} \tag{34}$$

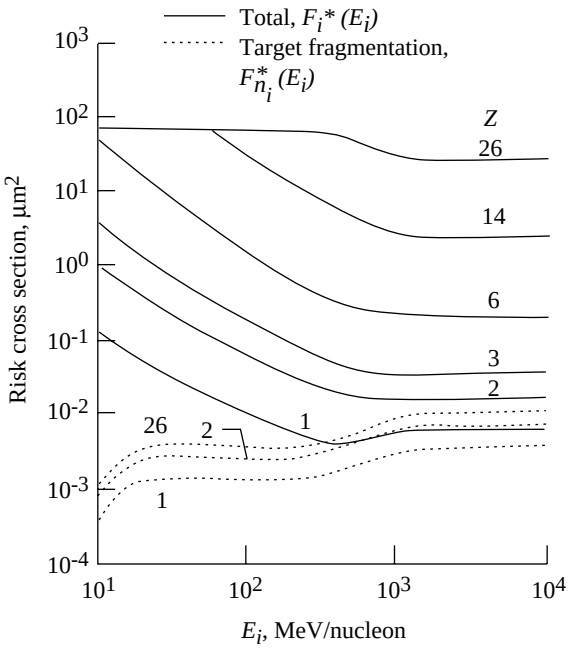

Figure 15. Risk cross section as function of particle energy for total contribution (ionization plus target fragmentation) and for target fragmentation contribution.

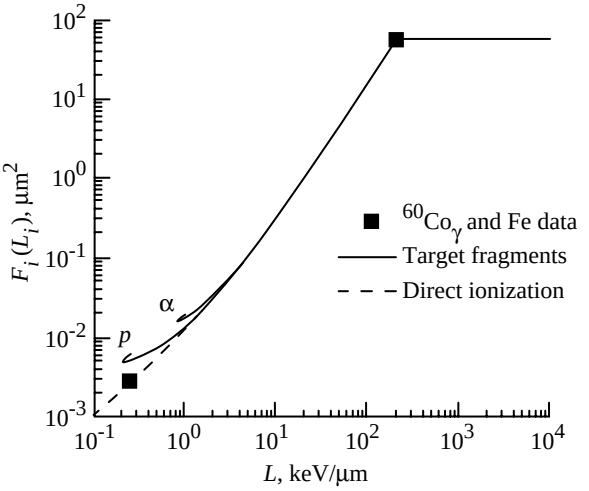

Figure 16. Risk cross section $F_i(L_i)$ for prevalence of Harderian gland tumor as function of LET used in calculations.

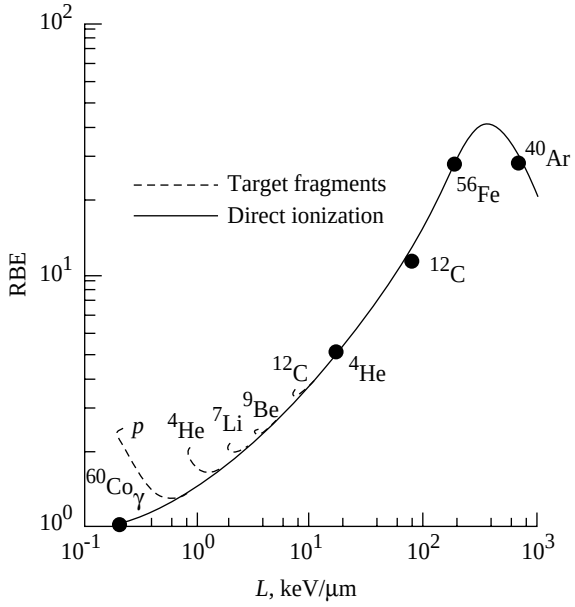

Figure 17. Relative biological effectiveness (RBE) for Harderian gland tumors including target fragment effects.

where A is the ion mass, E is the ion energy in units of MeV/amu, and L_i is the ion LET in keV/μm. The effective prevalence risk coefficient is shown in figure 16 for various ion components. The contribution from direct ionization is shown as the dashed curve. As yet, no known experimental data exist for proton exposures to test these nuclear fragment contributions to the prevalence risk coefficient. The effect of target fragmentation on RBE values is shown in figure 17 as the dashed extensions.

Cataract Index

A similar formalism has been developed for the formation of stationary cataracts in young rabbits. The risk coefficient for a stationary cataract index from direct ionization (Shinn et al. 1991) is taken as

$$F(L) = \left\{ \begin{array}{cc} 1.12 \times 10^{-2} L + 4 \times 10^{-4} L^2 & (L \leq 170 \text{ keV}/\mu\text{m}) \\ 13.5 & (L > 170 \text{ keV}/\mu\text{m}) \end{array} \right\} \tag{35}$$

and is shown in figure 18 in comparison with the data of Lett et al. (1988, 1989). Nuclear fragmentation contributions have been evaluated elsewhere (Shinn et al. 1991) and are shown in figure 19. The RBE of high-energy protons is calculated to be 1.4 in comparison with estimates from data for 2 GeV protons between 1 and 1.6 as estimated by Lett and Cox (from a private communication).

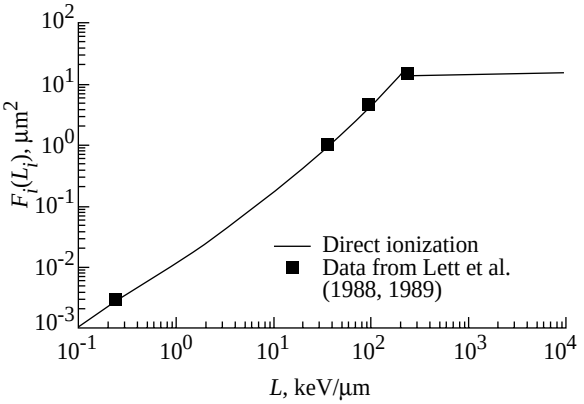

Figure 18. Fluence-based risk coefficient for intermediate phase of cataract index. Data points are from left-to-right $^{60}Co_\gamma$ and ^{20}Ne, ^{40}Ar, and ^{56}Fe ions.

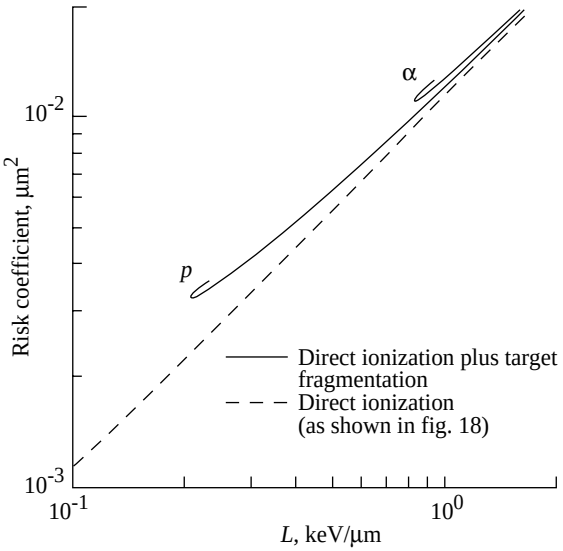

Figure 19. Effect of target fragmentation on risk coefficient for intermediate cataract.

Possible Effects in Human Cancer Response

In an earlier section, we evaluated the effects of target fragments on values of dose equivalent for various ions and found important contributions for light ions. We now consider the more complicated task of estimating their effects on protracted exposure with energetic ions. The complications arise since human cancer risk coefficients are mainly known for low-LET-exposure data with single exposures.

The lifetime excess cancer risk is given in NCRP 98 (Anon. 1989) for acute (2-day) exposure at age 35 as

$$R_a = 2.2 \times 10^{-2} H \left[1 + (H/1.16)\right] \tag{36}$$

with a similar result for a 10-year protracted exposure beginning at age 35 as

$$R_p = 1.8 \times 10^{-2} H \tag{37}$$

The dose equivalent is given as

$$H = Q(L) \; L \left[\phi_j(L)/6.24\right] \tag{38}$$

where $Q(L)$ is the quality factor, L is LET in keV/μm, and $\phi_j(L)$ is the type j particle fluence in number per μm^2. Two quality factors are considered as recommended by ICRP 26 (Anon. 1987) and ICRP 60 (Anon. 1991) as shown in figure 20. The corresponding fluence-based risk coefficients are

$$F_a\left(L,\phi_j\right) = R_a/\phi_j\left(L\right) \tag{39}$$

and

$$F_p\left(L,\phi_j\right) = R_p/\phi_j\left(L\right) \tag{40}$$

and are shown in figure 21 for the ICRP 26 quality factor and in figure 22 for the ICRP 60 quality factor. The acute fluence risk coefficient is taken as the "initial slope" value of equation (36). According to the prescription of NCRP 98 (Anon. 1989), the protracted exposure risk is 41 percent less than the acute exposure risk.

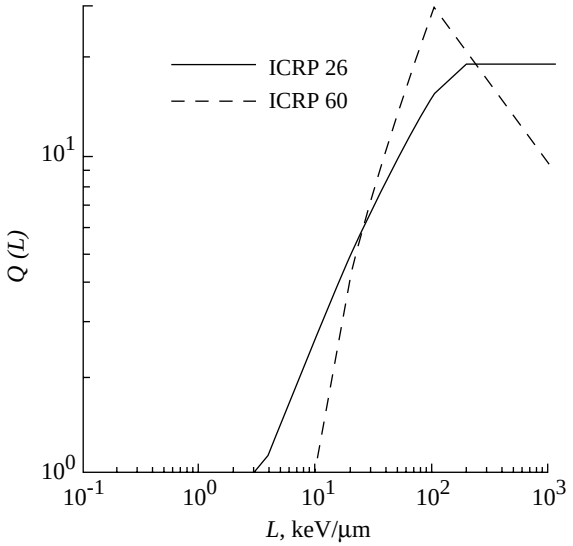

Figure 20. Quality factors defined by ICRP 26 and ICRP 60 (Anon. 1991).

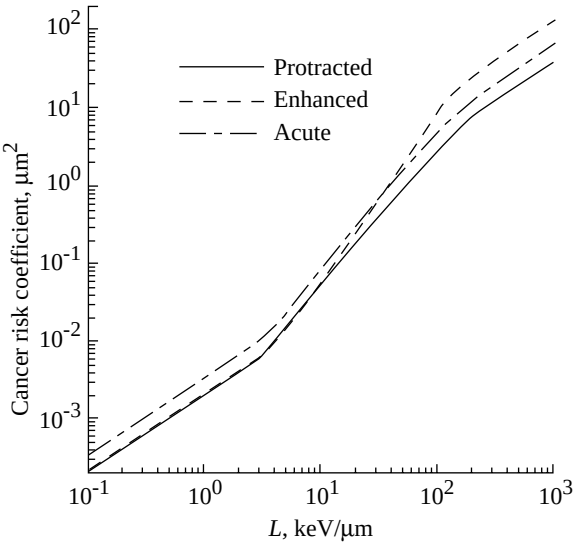

Figure 21. Excess cancer risk according to ICRP 26 and NCRP 98 (Anon. 1989).

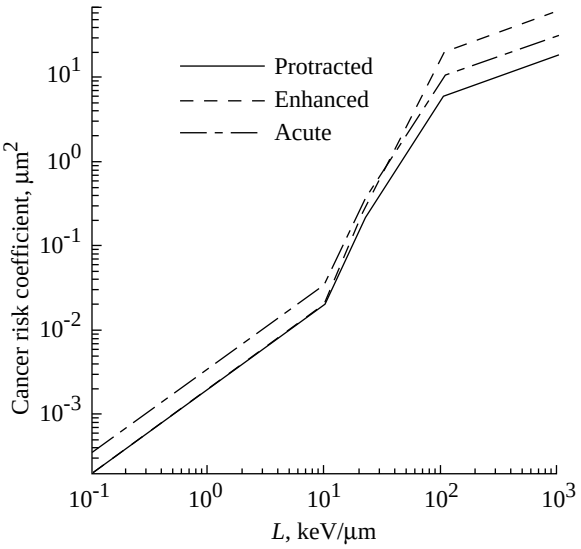

Figure 22. Excess cancer risk according to ICRP 60 and NCRP 98 (Anon. 1989).

A correct understanding on the use of these risk coefficients is found in how data are used to derive dose-related risk coefficients and quality factors. The risk coefficients are dominated by acute low-LET exposures of exposed individuals in the nuclear weapons blasts of World War II. The dose rate reduction factor is derived mainly from controlled animal experiments using X-ray or γ-ray exposures. The quality factor is derived by concensus of learned individuals based on measured RBE's for various biological systems and end points. The RBE is assumed to reach a maximum at low dose and/or dose rate on which quality factor is judged. One would assume that the quality factor is appropriate for low dose rate and that it generally overestimates for acute exposure. More recent evidence on life shortening in mice indicates a possible dose rate enhancement for high-LET exposures in the low dose region. This enhancement is indicated by the dashed curve in figures 21 and 22. Such enhancements are suggested to be the result of cell cycle effects (Rossi and Kellerer 1986) or, more simply, to be a property of the neutron response curve (Rossi 1981), or they may appear as repair-dependent phenomena.

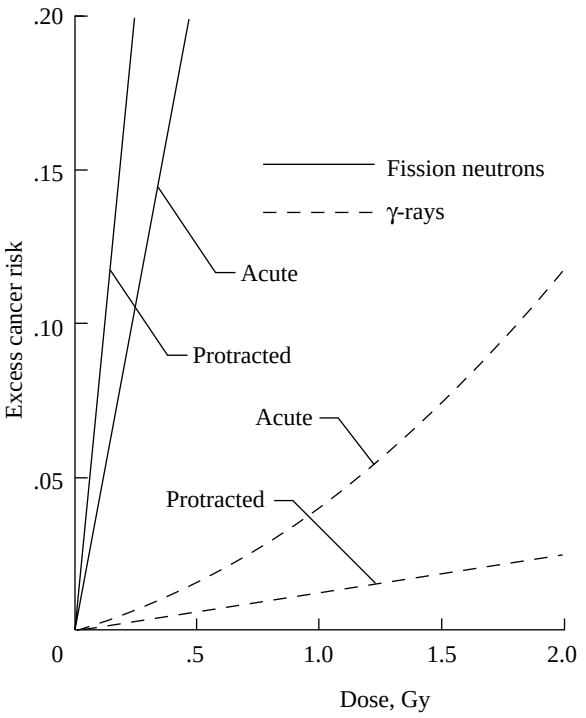

Figure 23. Excess cancer risk according to ICRP 60 (Anon. 1991) and NCRP 98 (Anon. 1989) assuming a quality factor of 20 for fission neutrons.

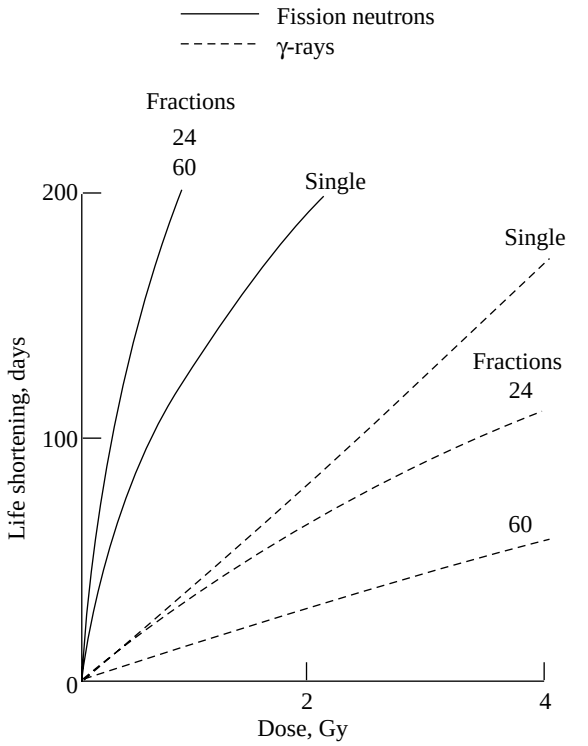

Figure 24. Life shortening in mice comparing exposure to neutrons with γ-irradiation for 24 or 60 fractions and for a single exposure. (Data are taken from Thomson et al. 1981–1989.)

Because life-shortening studies show that loss of life is enhanced by fractionation at high LET, we approximate the lifetime-cancer-risk cross section by twice the acute exposure values above 100 keV/μm. We assume that sparing is appropriate for the LET range for which $Q = 1$ (i.e., $L \leq 10$ keV/μm). A smooth connection is made between 10 and 100 keV/μm from the protracted cross section at low LET to twice the acute cross section at high LET. This is shown as the dashed curves in figures 21 and 22. The corresponding response curves are shown in figure 23 for γ-ray and fission neutron exposure ($Q \approx 20$). The relative values are similar to the life-shortening data in mice (Thomson et al. 1981–1989) as shown for comparison in figure 24.

The fission neutron curve is the same as that expected for relativistic Ar ions. We have calculated the cross section for direct ionization (according to NCRP 98 (Anon. 1989)) given as

$$F_a = \left\{ \begin{array}{ll} 3.5 \times 10^{-3} L & (L \leq 10) \\ 3.5 \times 10^{-3} L\,(0.32L - 2.2) & (10 \leq L \leq 100) \\ 1.06\sqrt{L} & (100 \leq L) \end{array} \right\} \tag{41}$$

with the corresponding protracted cross section assuming enhancement as

$$F_p = \left\{ \begin{array}{ll} 2.08 \times 10^{-3} L & (L \leq 10) \\ 2.08 \times 10^{-3} L\,(0.75 + 0.025L)\,(0.32L - 2.2) & (10 \leq L \leq 100) \\ 2.1\sqrt{L} & (100 < L) \end{array} \right\} \tag{42}$$

where L is LET in keV/μm. Note that equation (42) corresponds to the dashed curve in figure 22. The target fragment contributions are reasonably approximated by

$$F^*_{n,a}(E) = A^{0.4} \left\{ \frac{4.2 \times 10^{-4}}{1 + \exp\left[-(E - 12)/4.5\right]} + \frac{9.6 \times 10^{-4}}{1 + \exp\left[-(E - 700)/363\right]} \right\} \tag{43}$$

and provide a reasonable approximation to the nuclear effects in acute exposure.

In equation (43), A is the ion atomic weight and E is the kinetic energy in MeV/amu. The nuclear fragment effects on protracted exposure, assuming no dose rate enhancement, are also given by equation (43) if no repair occurs above 100 keV/μm. Assuming dose rate enhancement, the nuclear target fragment contribution is given as

$$F^*_{n,p}(E) = A^{8.4} \left\{ \frac{8.4 \times 10^{-4}}{1 + \exp\left[-(E - 12)/4.5\right]} + \frac{1.9 \times 10^{-3}}{1 + \exp\left[-(E - 700)/363\right]} \right\} \tag{44}$$

The fractional contribution of nuclear fragments (assuming dose rate enhancement) to the total-cancer-risk cross section is given in table 4. Significant target fragment contributions occur even for 100 MeV protons both to the acute exposure and especially to the protracted exposure assuming dose rate enhancement. The total cancer risk is dominated by target fragment contributions at high energy as shown in this table. The risk cross sections of various ions are shown in figures 25 and 26.

Table 4. Fraction of Nuclear Fragmentation Contribution to Total-Cancer-Risk Cross Section for Protons

	100 MeV	1000 MeV
$F^*_{n,a}/F^*_a$	0.14	0.66
F^*_{np}/F^*_p	.35	.85

The excess-cancer-risk coefficients per unit fluence are used in connection with the galactic cosmic ray (GCR) transport code HZETRN (Wilson, Townsend, and Badavi 1987) to evaluate astronaut risk to 1 year of GCR exposure protracted over a 10-year career. The results are given in table 5 for various particles (neutrons, protons, alphas, L (for $3 \leq Z \leq 9$), and H (for $10 \leq Z$)), as well as for the total exposure. The values given are according to the ICRP 60 quality factor (Anon. 1991) using the BEIR V risk data. The risk coefficient labeled *protracted* in figure 22 is used. The values of table 5 in parentheses assume dose rate enhancements at high LET and

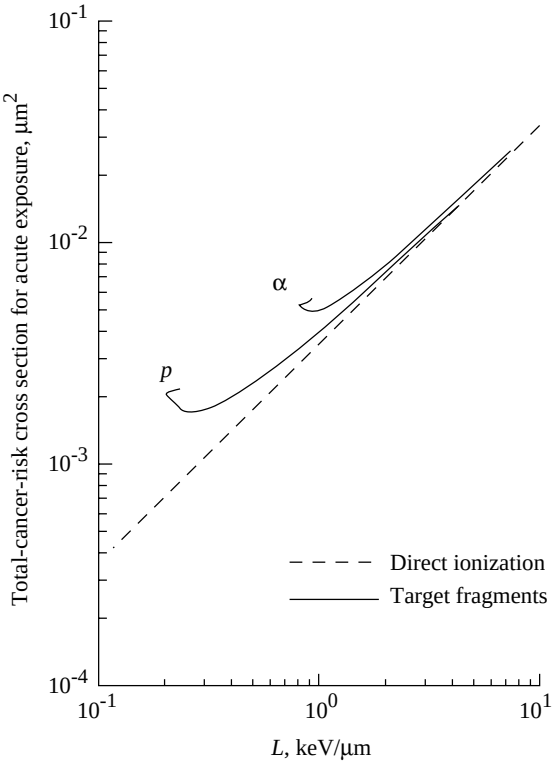

Figure 25. Acute-exposure-risk cross section for protons and alpha particles.

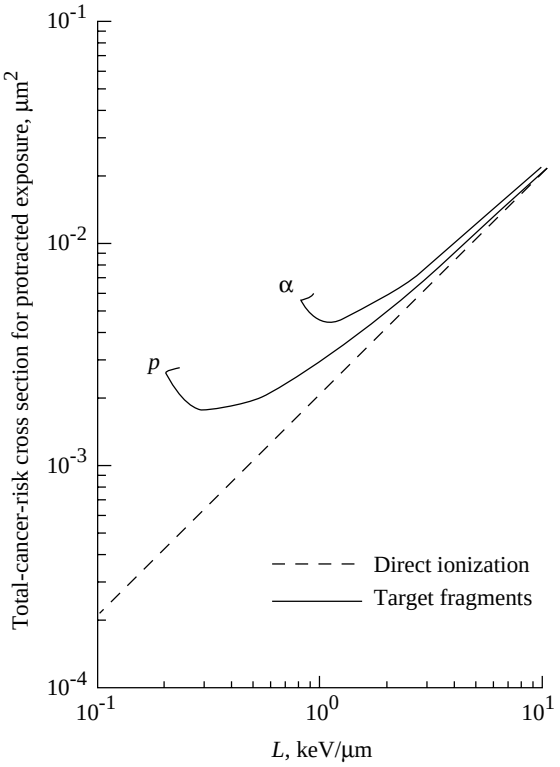

Figure 26. Protracted-exposure-risk cross section for protons and alpha particles.

Table 5. Excess Cancer Risk on Astronaut's Career for 1-Year Total Exposure Behind Aluminum Shielding Thickness

[Values in parentheses assume dose rate enhancement]

Aluminum shielding thickness, g/cm²	Excess cancer risk, percent, for—					
	n	*p*	*α*	*L*	*H*	Total
0	0 (0)	0.27 (0.51)	0.17 (0.24)	0.28 (0.53)	1.15 (2.90)	1.81 (4.17)
1	0 (.01)	.21 (.40)	.07 (.09)	.23 (.41)	1.00 (2.54)	1.52 (3.45)
2	.01 (.02)	.23 (.42)	.06 (.09)	.22 (.39)	.94 (2.34)	1.45 (3.25)
3	.01 (.03)	.24 (.43)	.06 (.09)	.21 (.36)	.86 (2.17)	1.38 (3.07)
5	.02 (.05)	.25 (.44)	.06 (.09)	.18 (.32)	.75 (1.87)	1.26 (2.76)
10	.03 (.08)	.27 (.45)	.05 (.08)	.14 (.24)	.54 (1.33)	1.00 (2.18)
15	.04 (.11)	.28 (.45)	.05 (.07)	.11 (.18)	.40 (.98)	.87 (1.80)
20	.05 (.13)	.28 (.45)	.04 (.06)	.08 (.14)	.30 (.74)	.75 (1.52)
30	.06 (.16)	.27 (.43)	.03 (.05)	.05 (.09)	.18 (.44)	.59 (1.15)
50	.06 (.18)	.23 (.36)	.02 (.03)	.02 (.04)	.07 (.17)	.41 (.77)

correspond to the risk coefficient labeled *protracted, enhanced* in figure 22. Note that the shield effectiveness depends on the risk model used. An aluminum shield of 15 g/cm^2 reduces the protracted risk by a factor of 2, whereas the protracted, enhanced risk is reduced by a factor of 2.3. We expect a strong dependence on shield material selection since high-LET components are strongly dependent on material composition (Wilson et al. 1991). None of the risk coefficients discussed herein are recommended for design studies, but the present study may be helpful in

defining the importance of the effects of dose rate enhancement in future recommended protection practices.

Concluding Remarks

In passing through a small region of tissue, the local energy deposit was shown to consist of direct ionization and excitation of electrons and energy given up to low-energy target fragments. The formalism was coupled to biological-related functions to evaluate the effects of target fragment contributions. In conventional risk assessment, the effective quality factor for high-energy protons is increased from its direct ionization value of 1 to 3.3 at 10 GeV. Experimental relative biological effectiveness (RBE) values between 1.4 and 4.4 have been observed for several biological systems for protons in the multi-GeV range.

Target fragmentation effects on track-structure models reveal a significant increase in proton RBE at low exposures. Such high RBE values result from the high efficiency of repair of X-ray-induced injury at low exposure and low dose rate. The predicted RBE is in good agreement with experiments for 160 MeV protons and Chinese hamster cells. Most of the injury from direct ionization of protons at low exposures is anticipated to be repaired at low exposures, and the main contribution to injury will result from target fragments for which repair is largely inhibited.

Significant contributions of target fragmentation are predicted for cancer induction in the Harderian gland and lesser contributions to cataract formation. No repair-dependent models exist for these systems. A simple repair-inhibited model is given for human cancer induction within which the inhibited repair of target fragment contributions further shows their importance for protracted exposures.

Fragmentation of target nuclei within biological systems has been shown to be an important contribution to light ion exposure. A primary concern is that direct ionization of light ions probably exhibits repair as an influence in radiation response, whereas the highly ionizing target fragments show little or no repair and may, in fact, exhibit enhanced risk at low exposure rates. Such factors have a potentially large impact on spacecraft shield design in future NASA missions.

NASA Langley Research Center
Hampton, VA 23681-0001
November 6, 1992

References

Alsmiller, R. G., Jr.; Armstrong, T. W.; and Coleman, W. A. 1970: *The Absorbed Dose and Dose Equivalent From Neutrons in the Energy Range 60 to 3000 MeV and Protons in the Energy Range 400 to 3000 MeV.* ORNL TM-2924, U.S. Atomic Energy Commission.

Anon. 1986: *The Quality Factor in Radiation Protection.* ICRU Rep. 40, International Commission on Radiation Units and Measurements.

Anon. 1987: *Recommendations of the International Commission on Radiological Protection.* ICRP Publ. 26, Pergamon Press Inc.

Anon. 1989: *Guidance on Radiation Received in Space Activities.* NCRP Rep. No. 98. National Council on Radiation Protection and Measurements.

Anon. 1991: *1990 Recommendations of the International Commission on Radiological Protection.* ICRP Publ. 60, Pergamon Press Inc.

Chatterjee, A.; Maccabee, H. D.; and Tobias, C. A. 1973: Radial Cutoff LET and Radial Cutoff Dose Calculations for Heavy Charged Particles in Water. *Radiat. Res.,* vol. 54, pp. 479–494.

Conklin, J. J.; and Hagan, M. P. 1987: Research Issues for Radiation Protection for Man During Prolonged Spaceflight. *Advances in Radiation Biology,* Volume 13, J. T. Lett, ed., Academic Press, Inc., pp. 215–284.

Cucinotta, Francis A.; Katz, Robert; Wilson, John W.; Townsend, Lawrence W.; Nealy, John E.; and Shinn, Judy L. 1991a: *Cellular Track Model of Biological Damage to Mammalian Cell Cultures From Galactic Cosmic Rays.* NASA TP-3055.

Cucinotta, Francis A.; Katz, Robert; Wilson, John W.; Townsend, Lawrence W.; Shinn, Judy L.; and Hajnal, Ferenc 1991b: Biological Effectiveness of High-Energy Protons: Target Fragmentation. *Radiat. Res.,* vol. 127, pp. 130–137.

Curtis, S. B.; Dye, D. L.; and Sheldon, W. R. 1965: Fractional Cell Lethality Approach to Space Radiation Hazards. *Second Symposium on Protection Against Radiations in Space,* Arthur Reetz, Jr., ed., NASA SP-71, pp. 219–223.

Curtis, S. B.; Townsend, L. W.; Wilson, J. W.; Powers-Risius, P.; Alpen, E. L.; and Fry, R. J. M 1992: Fluence-Related Risk Coefficients Using the Harderian Gland Data as an Example. *Adv. Space Res.,* vol. 12, no. 2–3, pp. (2)407–(2)416.

Diehl-Marshall, I.; and Bianchi, M. 1981: Induction of Micronuclei in Bean Roots by 250 GeV Hadrons. *Radiat. & Environ. Biophys.,* vol. 19, pp. 117–124.

Fry, R. J. M.; Powers-Risius, P.; Alpen, E. L.; and Ainsworth, E. J. 1985: High-LET Radiation Carcinogenesis. *Radiat. Res.,* vol. 104, pp. S-188–S-195.

Fry, R. J. M. 1986: Radiation Effects in Space. *Adv. Space Res.,* vol. 6, no. 11, pp. 261–268.

Gaubin, Y.; Planel, H.; Pianezzi, B.; Kovalev, E. E.; and Popov, V. I. 1979: Effects of 645 MeV and 9.2 GeV Protons on Artemia Eggs. *J. Radiat. Biol.,* vol. 36, no. 5, pp. 489–497.

Hall, Eric J.; Kellerer, Albrecht M.; Rossi, Harald H.; and Lam, Yuk-Ming P. 1978: The Relative Biological Effectiveness of 160 MeV Protons—II: Biological Data and Their Interpretation in Terms of Microdosimetry. *Int. J. Radiat. Oncol. Biol. Phys.,* vol. 4, no. 11 & 12, Nov.–Dec., pp. 1009–1013.

Katz, R.; Ackerson, B.; Homayoonfar, M.; and Sharma, S. C. 1971: Inactivation of Cells by Heavy Ion Bombardment. *Radiat. Res.,* vol. 47, pp. 402–425.

Katz, Robert; Sharma, S. C.; and Homayoonfar, M. 1972: The Structure of Particle Tracks. *Topics in Radiation Dosimetry, Supplement 1,* F. H. Attix, ed., Academic Press, Inc., pp. 317–383.

Katz, Robert 1986: Biological Effects of Heavy Ions From the Standpoint of Target Theory. *Adv. Space Res.,* vol. 6, no. 11, pp. 191–198.

Katz, Robert; and Cucinotta, F. A. 1991: RBE vs. Dose for Low Doses of High-LET Radiations. *Health Phys.,* vol. 60, pp. 717–718.

Kellerer, A. M.; and Chmelevsky, D. 1975: Criteria for Applicability of LET. *Radiat. Res.,* vol. 63, pp. 226–234.

Lett, J. T.; Cox, A. B.; and Lee, A. C. 1988: Selected Examples of Degenerative Late Effects Caused by Particulate Radiations in Normal Tissues. *Terrestrial Space Radiation and Its Biological Effects,* Percival D. McCormack, Charles E. Swenberg, and Horst Bucker, eds., Plenum Press, pp. 393–413.

Lett, J. T.; Lee, A. C.; Cox, A. B.; and Wood, D. H. 1989: Late Cataractogenesis Caused by Particulate Radiations and Photons in Long-Lived Mammalian Species. *Adv. Space Res.,* vol. 9, no. 10, pp. (10)325–(10)331.

Lindstrom, P. J.; Greiner, D. E.; Heckman, H. H.; Cork, Bruce; and Bieser, F. S. 1975: *Isotope Production Cross Sections From the Fragmentation of* ^{16}O *and* ^{12}C *at Relativistic Energies.* LBL-3650 (NGR-05-003-513), Lawrence Berkeley Lab., Univ. of California.

Mathews, G. J. 1983: Complete Fragment Yields From Spallation Reactions Via a Combined Time-of-Flight and ΔE-E Technique. *Composition and Origin of Cosmic Rays,* Maurice M. Shapiro, ed., Kluwer Academic Publ., pp. 317–320.

Paretzke, Herwig G. 1988: Problems in Theoretical Track Structure Research for Heavy Charged Particles. *Quantitative Mathematical Models in Radiation Biology,* Jürgen Kiefer, ed., Springer-Verlag, pp. 49–56.

Rossi, Harald H. 1981: Considerations on the Time Factor in Radiobiology. *Radiat. & Environ. Biophys.,* vol. 20, pp. 1–9.

Rossi, H. H.; and Kellerer, A. M. 1986: The Dose Rate Dependence of Oncogenic Transformation by Neutrons May be Due to Variation of Response During the Cell Cycle. *Int. J. Radiat. & Biol.,* vol. 50, no. 2, pp. 353–361.

Shinn, J. L.; Wilson, J. W.; and Ngo, D. M. 1990: Risk Assessment Methodologies for Target Fragments Produced in High-Energy Nucleon Reactions. *Health Phys.,* vol. 59, no. 1, pp. 141–143.

Shinn, J. L.; Wilson, J. W.; Cox, A. B.; and Lett, J. T. 1991: A Study of Lens Opacification for a Mars Mission. SAE Tech. Paper Ser. 911354.

Silberberg, R.; Tsao, C. H.; and Shapiro, M. M. 1976: Semiempirical Cross Sections, and Applications to Nuclear Interactions of Cosmic Rays. *Spallation Nuclear Reactions and Their Applications,* B. S. P. Shen and M. Merker, eds., D. Reidel Publ. Co., pp. 49–81.

Silberberg, R.; Tsao, C. H.; and Letaw, John R. 1983: Improvement of Calculations of Cross Sections and Cosmic-Ray Propagation. *Composition and Origin of Cosmic Rays,* Maurice M. Shapiro, ed., D. Reidel Publ. Co., pp. 321–336.

Smith, Harold H. 1967: Relative Biological Effectiveness of Different Types of Ionizing Radiations: Cytogenetic Effects in Maize. *Radiat. Res.,* suppl. 7, pp. 190–195.

Thomson, John F.; Williamson, Frank S.; Grahn, Douglas; and Ainsworth, E. John 1981a: Life Shortening in Mice Exposed to Fission Neutrons and γ Rays. I. Single and Short-Term Fractionated Exposures. *Radiat. Res.,* vol. 86, pp. 559–572.

Thomson, John F.; Williamson, Frank S.; Grahn, Douglas; and Ainsworth, E. John 1981b: Life Shortening in Mice Exposed to Fission Neutrons and γ Rays. II. Duration-of-Life and Long-Term Fractionated Exposures. *Radiat. Res.,* vol. 86, pp. 573–579.

Thomson, John F.; Williamson, Frank S.; and Grahn, D. 1983: Life Shortening in Mice Exposed to Fission Neutrons and γ Rays. III. Neutron Exposures of 5 and 10 Rad. *Radiat. Res.,* vol. 93, pp. 205–209.

Thomson, John F.; Williamson, Frank S.; and Grahn, Douglas 1985a: Life Shortening in Mice Exposed to Fission Neutrons and γ Rays. IV. Further Studies With Fractionated Neutron Exposures. *Radiat. Res.,* vol. 103, pp. 77–88.

Thomson, John F.; Williamson, Frank S.; and Grahn, Douglas 1985b: Life Shortening in Mice Exposed to Fission Neutrons and γ Rays. V. Further Studies With Single Low Doses. *Radiat. Res.,* vol. 104, pp. 420–428.

Thomson, John F.; Williamson, Frank S.; and Grahn, Douglas 1986: Life Shortening in Mice Exposed to Fission Neutrons and γ Rays. VI. Studies With the White-Footed Mouse, Peromyscus Leucopus. *Radiat. Res.,* vol. 108, pp. 176–188.

Thomson, John F.; and Grahn, Douglas 1988: Life Shortening in Mice Exposed to Fission Neutrons and γ Rays. VII. Effects of 60 Once-Weekly Exposures. *Radiat. Res.,* vol. 115, pp. 347–360.

Thomson, John F.; and Grahn, Douglas 1989: Life Shortening in Mice Exposed to Fission Neutrons and γ Rays. VIII. Exposures to Continuous γ Radiation. *Radiat. Res.,* vol. 118, pp. 151–160.

Todd, Paul Wilson 1964: Reversible and Irreversible Effects of Ionizing Radiations on the Reproductive Integrity of Mammalian Cells Cultured In Vitro. Ph.D. Thesis, Univ. of California.

Townsend, L. W.; Wilson, J. W.; and Bidasaria, H. B. 1982: On the Geometric Nature of High-Energy Nucleus-Nucleus Reaction Cross Sections. *Canadian J. Phys.,* vol. 60, no. 10, pp. 1514–1518.

Townsend, Lawrence W.; Wilson, John; and Cucinotta, Francis A. 1987: A Simple Parameterization for Quality Factor as a Function of Linear Energy Transfer. *Health Phys.,* vol. 53, no. 5, pp. 531–532.

Waligórski, M. P. R.; Sinclair, G. L.; and Katz, R. 1987: Radiosensitivity Parameters for Neoplastic Transformations in C3H10T1/2 Cells. *Radiat. Res.,* vol. 111, pp. 424–437.

Wilson, John W. 1977: *Analysis of the Theory of High-Energy Ion Transport.* NASA TN D-8381.

Wilson, John W.; Stith, John J.; and Stock, L. V. 1983: *A Simple Model of Space Radiation Damage in GaAs Solar Cells.* NASA TP-2242.

Wilson, John W.; Townsend, L. W.; Bidasaria, H. B.; Schimmerling, Walter; Wong, Mervyn; and Howard, Jerry 1984: ^{20}Ne Depth-Dose Relations in Water. *Health Phys.,* vol. 46, no. 5, pp. 1101–1111.

Wilson, J. W.; Townsend, L. W.; and Badavi, F. F. 1987: Galactic HZE Propagation Through the Earth's Atmosphere. *Radiat. Res.,* vol. 109, no. 2, pp. 173–183.

Wilson, John W.; Chun, S. Y.; Buck, W. W.; and Townsend, L. W. 1988: High Energy Nucleon Data Bases. *Health Phys.,* vol. 55, no. 5, pp. 817–819.

Wilson, John W.; Townsend, Lawrence W.; and Khan, Ferdous 1989: Evaluation of Highly Ionizing Components in High-Energy Nucleon Radiation Fields. *Health Phys.,* vol. 57, no. 5, pp. 717–724.

Wilson, John W.; Townsend, Lawrence W.; Nealy, John E.; Hardy, Alva C.; Atwell, William; and Schimmerling, Walter 1991a: *Preliminary Analysis of a Radiobiological Experiment for LifeSat.* NASA TM-4236.

Wilson, John W.; Townsend, Lawrence W.; Schimmerling, Walter; Khandelwal, Govind S.; Khan, Ferdous; Nealy, John E.; Cucinotta, Francis A.; Simonsen, Lisa C.; Shinn, Judy L.; and Norbury, John W. 1991b: *Transport Methods and Interactions for Space Radiations.* NASA RP-1257.

Yang, Tracy Chui-Hsu; Craise, Laurie M.; Mei, Man-Tong; and Tobias, Cornelius A. 1985: Neoplastic Cell Transformation by Heavy Charged Particles. *Radiat. Res.,* vol. 104, pp. S-177–S-187.

REPORT DOCUMENTATION PAGE

Form Approved
OMB No. 0704-0188

1. AGENCY USE ONLY *(Leave blank)*	2. REPORT DATE	3. REPORT TYPE AND DATES COVERED
	February 1993	Technical Memorandum

4. TITLE AND SUBTITLE
Target Fragmentation in Radiobiology

5. FUNDING NUMBERS
WU 199-04-16-11

6. AUTHOR(S)
John W. Wilson, Francis A. Cucinotta, Judy L. Shinn,
and Lawrence W. Townsend

7. PERFORMING ORGANIZATION NAME(S) AND ADDRESS(ES)
NASA Langley Research Center
Hampton, VA 23681-0001

8. PERFORMING ORGANIZATION REPORT NUMBER
L-17138

9. SPONSORING/MONITORING AGENCY NAME(S) AND ADDRESS(ES)
National Aeronautics and Space Administration
Washington, DC 20546-0001

10. SPONSORING/MONITORING AGENCY REPORT NUMBER
NASA TM-4408

11. SUPPLEMENTARY NOTES
This work was presented at the Investigators Meeting on Space Radiation Research, Houston, TX, Apr. 22–23, 1991.

12a. DISTRIBUTION/AVAILABILITY STATEMENT
Unclassified–Unlimited

Subject Category 52

12b. DISTRIBUTION CODE

13. ABSTRACT *(Maximum 200 words)*
Nuclear reactions in biological systems produce low-energy fragments of the target nuclei seen as local high events of linear energy transfer (LET). A nuclear-reaction formalism is used to evaluate the nuclear-induced fields within biosystems and their effects within several biological models. On the basis of direct ionization interaction, one anticipates high-energy protons to have a quality factor and relative biological effectiveness (RBE) of unity. Target fragmentation contributions raise the effective quality factor of 10 GeV protons to 3.3 in reasonable agreement with RBE values for induced micronuclei in bean sprouts. Application of the Katz model indicates that the relative increase in RBE with decreasing exposure observed in cell survival experiments with 160 MeV protons is related solely to target fragmentation events. Target fragment contributions to lens opacity give an RBE of 1.4 for 2 GeV protons in agreement with the work of Lett and Cox. Predictions are made for the effective RBE for Harderian gland tumors induced by high-energy protons. An exposure model for lifetime cancer risk is derived from NCRP 98 risk tables, and protraction effects are examined for proton and helium ion exposures. The implications of dose rate enhancement effects on space radiation protection are considered.

14. SUBJECT TERMS	15. NUMBER OF PAGES
Nuclear fragments; Biological response; Cancer	24
	16. PRICE CODE: A03

17. SECURITY CLASSIFICATION OF REPORT	18. SECURITY CLASSIFICATION OF THIS PAGE	19. SECURITY CLASSIFICATION OF ABSTRACT	20. LIMITATION OF ABSTRACT
Unclassified	Unclassified		